Journal of Environment and Earth Science
ISSN 2224-3216 (Paper) ISSN 2225-0948 (Online)
Vol. 3, No.12, 2013

Mapping of Hydrothermal Alteration in Mount Berecha Area of Main Ethiopian Rift using Hyperspectral Data

Ayomiposi G. Oluwadebi[1], Christoph A. Hecker[2], Freek D. van der Meer[2], Graham Ferrier [3]

1. Department of Geological Sciences, Osun State University, Osogbo, Osun State, Nigeria
2. Department of Earth Systems Analysis, Faculty of Geo-Information Science and Earth Observation (ITC), University of Twente, Enschede, Netherlands
3. Department of Geography, Environment and Earth Sciences, University of Hull, United Kingdom

* E-mail of the corresponding author: ayomiposi.oluwadebi@uniosun.edu.ng

Abstract
Airborne Imaging Spectroradiometer for Applications (AISA) Hawk data was used to identify and map hydrothermal alteration mineralogy in Mount Berecha area of Main Ethiopian Rift valley. The Airborne image mapping was coupled with laboratory analysis involving reflectance spectroscopic measurements with the use of ASD FieldSpec for mineral and rock samples. The study was based in the shortwave infrared wavelength (SWIR) region. Laboratory spectra acquired from field data analysis served as guide in selecting image endmembers which were used as input in Spectral Angle Mapper (SAM) classification for mineral mapping. SWIR spectroscopy was able to detect the main very fine grained mineral assemblages which occur in the study area, including kaolinite, halloysite, opal, montmorillonite, nontronite, calcite, K-alunite, palygorskite, MgChlorite, zoisite, illite and mixtures of these minerals. SAM classification algorithm gives the overall classification of the alteration minerals of Berecha area and was used to generate the surficial mineral map of the study area. Berecha alteration is related to low sulfidation system and the most widespread alteration effects are represented essentially in advanced argillic alteration assemblage consisting mainly of kaolinite + opal + smectite $\pm$ alunite which is likely of steam heated origin.
Keywords: Hyperspectral, Imaging Spectrometry, AISA Hawk, Berecha, ASD FieldSpec, Spectral Angle Mapper

1. Introduction

Hydrothermal alteration is a complex process involving chemical replacement of original minerals in the rock by new minerals where a hydrothermal fluid delivers the chemical reactants and remove the aqueous reaction products (Reed, 1997). An understanding of hydrothermal alteration is of great value because it provides insight into origin of ore fluids as well as chemical and physical attributes of ore (deposit) formation. Gold and many other economic mineralizations in the world have been found in alteration zones. Mount Berecha area of the Main Ethiopia Rift (MER) is a typical example of hydrothermally altered area. The occurrence of gold in various part of Ethiopia is known to be associated with the metamorphic rocks (green schist facies & amphibolites facies), low-grade bimodal meta-volcano sedimentary island-arc (ophiolitic suites) and syn-tectonic to post-tectonic intrusive (Tadesse, 1999, Tadesse et al., 2003). However, recent studies show elevated gold values in geothermal wells in hydrothermally altered areas of Ethiopian rift system. This work is based on identifying the alteration mineralogy in the study area and the possibility of gold at the surface or occurrence of other important economic mineral. An airborne hyperspectral dataset (Hawk data) was used to make a mineral map of Mount Berecha area hydrothermal system and then ground-truthed with the use of ASD FieldSpec. Airborne Imaging Spectroradiometer for Applications (AISA) Hawk is a commercial hyperspectral push broom type imaging spectrometer system developed by SPECIM based in Finland (van der Meer, 2001). The flight campaign of the study area was carried out in January 2008 by NERC-ARSF (National Environmental Research Council – Airborne Research and Survey Facility) based in United Kingdom.

Spectroscopy is the measurement and analysis of portions of the electromagnetic spectrum to identify spectrally distinct and physically significant features of a material (Thomas and Walter, 2002). Most minerals have a characteristic spectrum and major diagnostic absorption feature between the wavelength ranges of 1300-2500 nm (SWIR) range (van der Meer et al., 2012). The majority of the spectral absorption features that distinguish different silicates is associated with hydroxyl and water, producing absorption features near 1400nm (OH and water) and 1900nm (water). Other important and diagnostic spectral absorption features occur at or near 2200nm, 2250nm and 2330 and are related to the bending and stretching of the bonds between AlOH, FeOH and MgOH respectively (Figure 1). The absorption features that denote these hydroxyl- and carbonate-bearing minerals or mineral groups are characteristic of hydrothermal alteration. These mineral groups may include kaolinite, halloysite, pyrophyllite, smectite clays, dickite, micas, chlorites, alunite, jarosite, calcite (Pontual et al., 1997).

Journal of Environment and Earth Science
ISSN 2224-3216 (Paper) ISSN 2225-0948 (Online)
Vol. 3, No.12, 2013

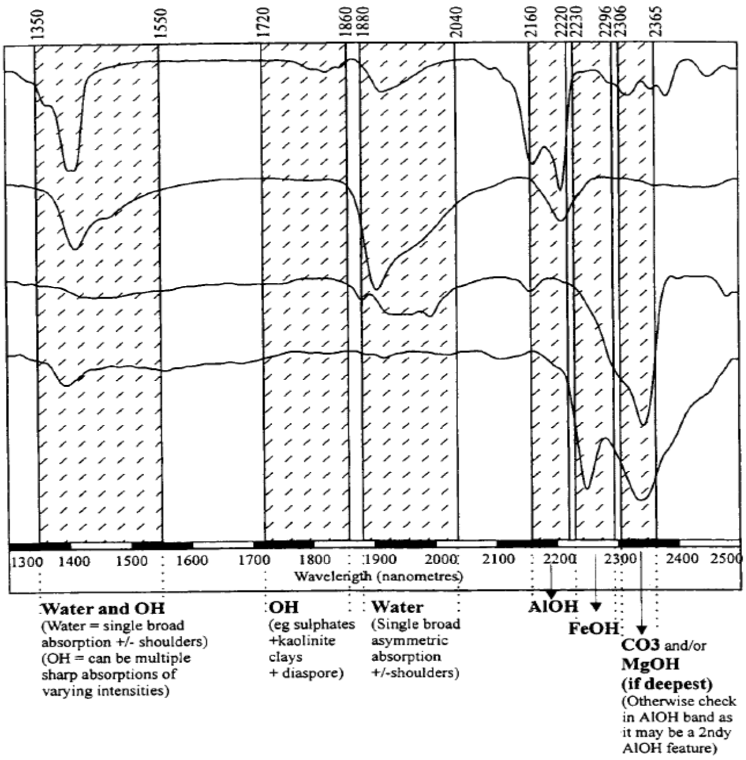

Figure 2: Major spectral absorption band in SWIR (Pontual et al., 1997)

2. Geologic Setting

Mount Berecha area is situated in the central part of the Main Ethiopian Rift (MER) valley near the city of Abaya (Figure 2). The Main Ethiopia Rift (MER) constitute the north-eastern part of the East African Rift System (EARS) and comprises a series of rift zones extending over a distance of about 1000 km from the Afar Triple Junction at the Red Sea-Gulf of Aden intersection to the Kenya Rift (Abebe et al., 2007). The MER is marked by recent volcanic products (rocks) which are represented by composite volcanoes and by caldera structures (Boccaletti et al., 1998). The MER developed during Late Miocene and characterized by well-developed Quaternary faulting that is mostly related to Wonji Fault Belt (Korme et al., 2004). The MER is divided geographically into three sectors: northern, central and southern (WoldeGabriel et al., 1990). The study area(Berecha) exists in the central part of the Main Ethiopian Rift valley which is mostly covered by ignimbrite rock (Dipaola, 1970). Berecha ignimbrite is the youngest unit out of the three ignimbritic units of the volcanic complex that belongs to a bimodal magmatic suite erupted between 830 Ka and 20 Ka (thousand years)(Trua et al., 1999). The recent felsic products of the Berecha unit consist of pantelleritic ignimbrites and obsidian lava domes and flows ranging from 240 - 20 Ka. The pyroclastics are unwelded pumice flows and ashes, which are the final products (Boccaletti et al., 1999). Berecha area consist of Pleistocene – Holocene (<1.6 Ma) volcanic complex with volcano-sedimentary rocks which is Recent (< 500 Ka) (Tsegaye et al., 2005). The geology map of Berecha area is shown in Figure 3.

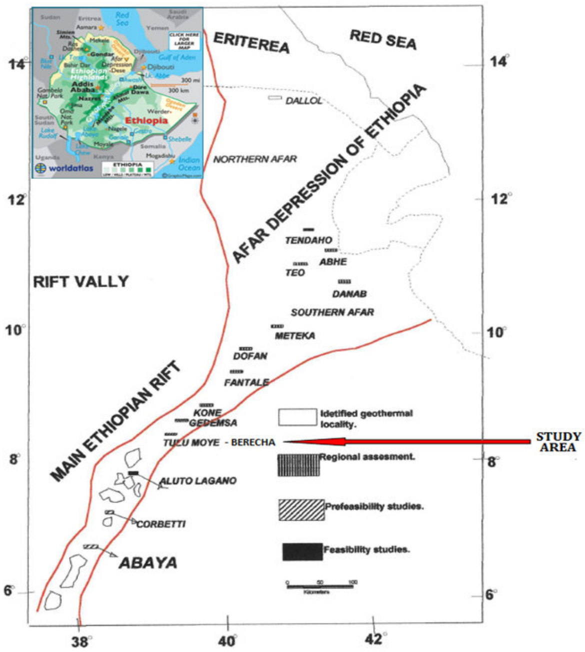

Figure 3: Map of Main Ethiopian Rift showing study area after (Ayele et al., 2002)

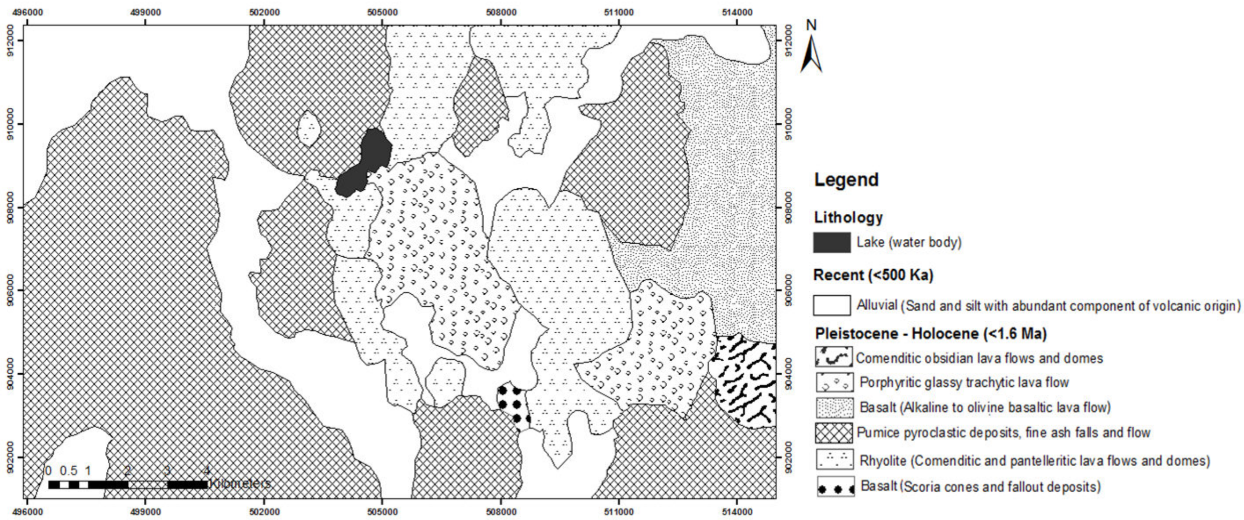

Figure 3: Geology map of Berecha area after (Tsegaye et al., 2005)

3. Methodology

3.1 Ground Data

Samples of mineral and rock were collected from eighty-three (83) sampling points (locations) with their GPS readings. Sampling was carried out in two ways, random sampling which was done by random collection of samples from altered part of the study area and detailed sampling which was based on information obtained from preliminary processing (wavelength mapping) of airborne imagery (AISA Hawk data) which shows variability in colour indicating different alteration minerals. Laboratory spectra of mineral and rock were acquired using ASD (Analytical Spectral Device) FieldSpec with the high intensity contact probe instrument (Arthur, 2007). ASD FieldSpec is a full computer-controlled spectroradiometer with a spectral range of 350 - 2500 nm (Figure 4). It is designed to collect solar reflectance, radiance and irradiance measurements of materials. ASD

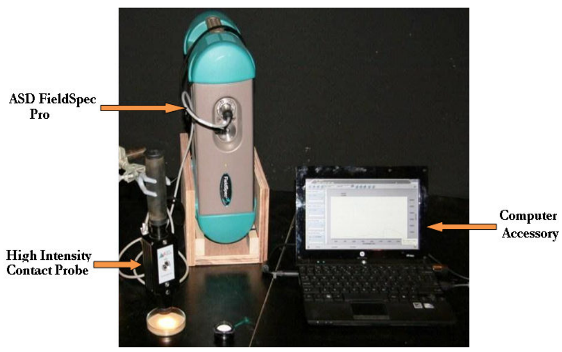

Figure 4: ASD FieldSpec Diagram

FieldSpec is compact and easy to set up, thus allowing much data collection. The instrument has a contact reflectance probe, which can be fixed to the fibre-optic cable to provide spectral capabilities measurement without the need for sunlight. This attachment brings the ASD FieldSpec in line with other instruments such as the PIMA SP, allowing collection of high quality reflectance spectra over a range of surfaces, with improved signal to noise ratios, thus making it ideal for spectral library creation. The laboratory spectra acquired were processed visually using ViewSpecPro software and further analyzed with "The Spectral Geologist" (TSG) software (CSIRO, 2010). This is specialized software designed for spectra analysis and interpretation. It provides automated assistance in spectral interpretation by comparing sampled spectra with extensive spectral libraries. TSG is not perfect in mineral identification, certain degree of error is possible and this was taken into consideration during analysis.

3.2 Airborne data

The AISA Hawk data was newly obtained, thus it involved some pre-processing steps before different mapping techniques were employed. The aim for processing was to identify hydrothermal alteration assemblage and highlight end-member relationship. The AISA Hawk records the SWIR range between 1006 nm and 2457 nm and it is accompany by AISA Eagle which covers the VIS-VNIR range between 393 and 988 nm (Table 1 shows specification of the AISA Hawk). AISA Hawk data was used in this study due to its SWIR region spectral coverage that is of interest in alteration mineral mapping.

Table 2: AISA Hawk Sensor Specification

Spectral Range	1006 - 2457 nm
Sampling Interval	6.3 nm
Spectral Band	252
Spectral Resolution	12 nm
Altitude amsl	12000 feet
Pixel size	2.5 m
IFOV	0.075 degree
Ground IFOV at 2000 m flying height	2.62 m

Processing was performed using ENVI 4.7 software (ENvironment for Visualizing Images), which is specifically designed for image processing of satellite and aircraft remote-sensing hyperspectral data. ENVI is suitable for processing hyperspectral data because of its many unique interactive analysis tools and multiple dynamic overlay capabilities. It also allows users to make and apply their own customized analysis strategies. Image endmembers were identified by using the laboratory spectra acquired from field data as guide in picking pixels with pure endmember spectra from the pre-processed image. The image derived endmembers were compared with USGS spectra library to check their similarity in absorption features and shape. These (image derived endmembers) also serves as the training set (input) in Spectral Angle Mapper (SAM) classification, (Hecker et al., 2008) which was used to generate the mineral map. SAM is a tool that permits rapid mapping of the spectra similarity of image spectra to reference spectra. The algorithm determines the spectral similarity between test reflectance spectrum and reference reflectance spectrum by calculating the "angle" between the two spectra, treating them as vectors in a space with dimensionality equal to the number of bands assuming that the data is correctly calibrated to apparent reflectance with dark current path and radiance removed (Kruse et al., 1993).

4. Results And Discussion

4.1 Ground Data

Classification made by The Spectral Geologist software from the laboratory spectral of minerals and rocks show the presence of several shortwave infrared wavelength (SWIR) active alteration minerals which include: kaolinite and halloysite (kandite group minerals), montmorillonite and nontronite (smectite group mineral), opal, calcite, k-alunite, palygorskite, mgchlorite, zoisite, illite and mixtures of these minerals. Some of the samples have pure spectra of the mineral identified (e.g. kaolinite, opal etc); others however occur as mixture with other mineral without pure spectra to describe their spectral features (these include palygorskite, mgchlorite, zoisite, illite). Some of the samples with distinct (pure) spectral compared with USGS spectra library are shown in Figure 5.

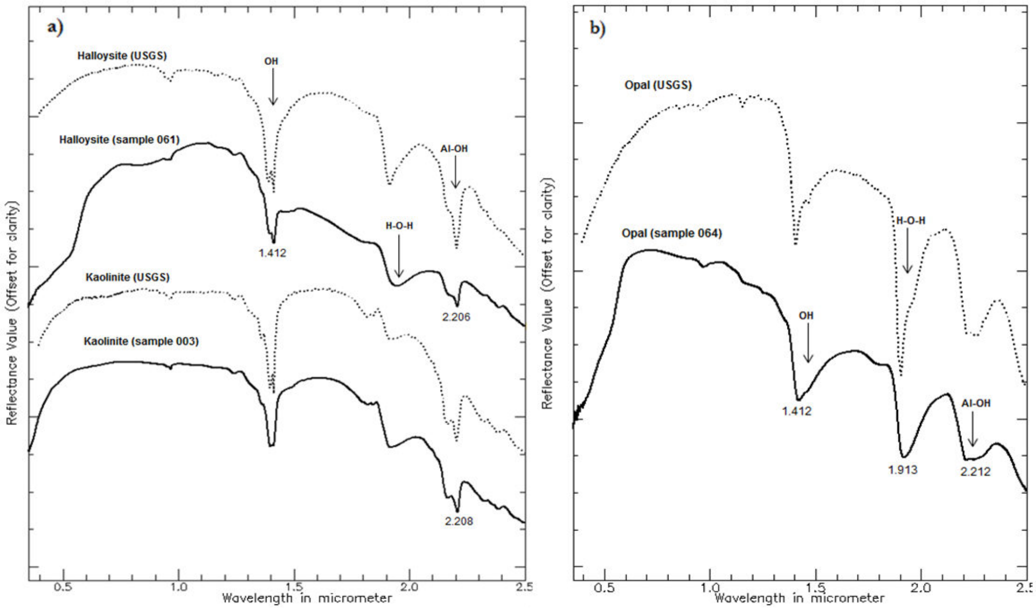

Figure 5: Laboratory spectra of minerals compared with USGS Library spectra: (a) Kaolinite and Halloysite spectral (b) Opal spectral

The alteration minerals are unevenly distributed over the study area. Kaolinite dominates other alteration minerals which covers larger part of the area. It exists as pure spectra in some cases and as mixed spectra with other minerals in most cases. Next to kaolinite is opal and smectite group (montmorillonite and nontronite) occur sparsely within the study area. Calcite and k-alunite occur in few samples analyzed, while palygorskite, mgchlorite, zoisite and illite occurs as mixture with other minerals and are poorly distributed in the area.

Figure (6a) show an overview of the mineral distribution in the area using field observation points overlay on geology map of the study area. Major part of the alteration is associated with the Pleistocene - Holocene rhyolite felsic rock and some occurring on pumice pyroclastic deposits and on trachyte lithogical unit with fewer occurrence in the volcano-sedimentary lithological units. This infers that alteration in the study area is associated with bimodal (rhyolite and basalt) volcanic rocks. The pattern of mineral occurrence was revealed better from the portion of the area where detailed study was carried out (Figure 6b). Minerals with similar composition often occur together as found in the case of kaolinite and halloysite and vice versa. Mineral-1 indicates the most occurring mineral in a sample while mineral-2 is the next mineral abundance and mineral-3 appear when there are up to three minerals in the sample. Some samples have just a mineral in the sample analyzed

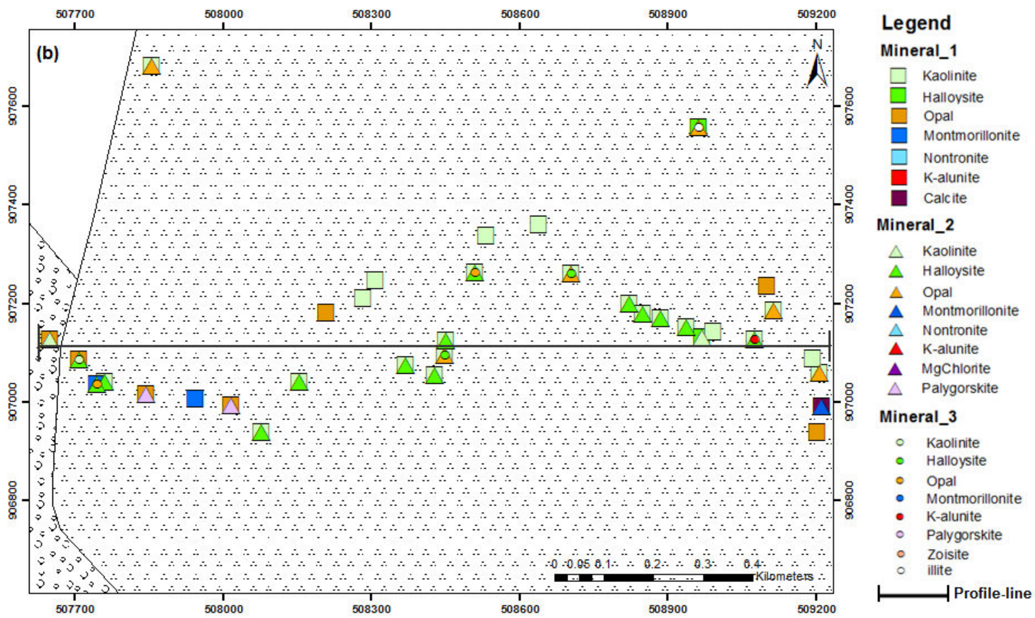

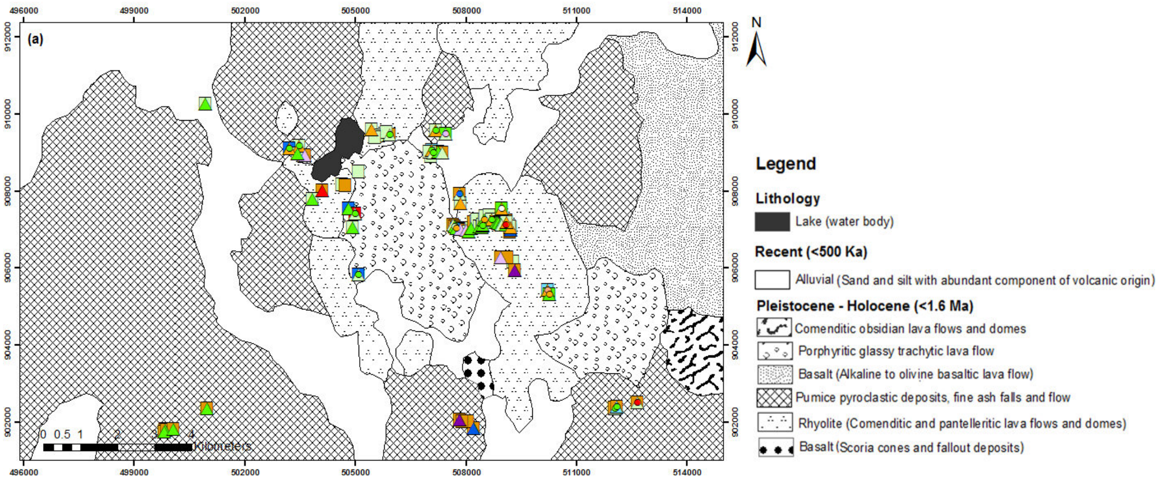

Figure 6: (a) Mineral distribution in the study area overlay on Geology map; (b) Profile section of detailed study area

4.2 Airborne Data

Eight groups of endmembers were identified from the image (Figure 7). Kaolinite spectrum is clearly seen in few area of the image while in many case, it occur as mixed spectra. Therefore, due to impurity of the pixels, two endmembers were selected for kaolinite [i.e. kaolinite (a) and kaolinite (b)] in order to obtain good classification result. Halloysite and kaolinite which are both kandite mineral group are found in association with each other with main absorption feature at 2.217 µm, they are group together as halloysite endmember. Other endmembers as shown in the figure have their own diagnostic absorption features as well as spectral shape to differentiate them from others. The endmember named "agricultural field" have absorption feature similar to that of nontronite and calcite but was classified as agricultural field area in the SAM classification because it was confirmed during ground truthing that those areas were used for agricultural purpose. Another endmember of unknown mixed spectra also exist in the image in which diagnostic double absorption feature of Al-OH was noticed in some of the pixels at 2.192 µm and 2.217 µm and it is similar to alunite absorption feature but other diagnostic absorption feature of alunite were absent, therefore the group was not considered as alunite but grouped as unknown mixed spectra. The abundances of two kaolinite end-members show that although they occur together in most cases, they also occur separately and delineate different features. The features are interpreted as being caused by hydrothermal fluids rather than weathering because they indicate typical hydrothermal mineral associations. Kaolinite crystallinity study was also carried out to confirm that the kaolinite in the study area is of hydrothermal origin.

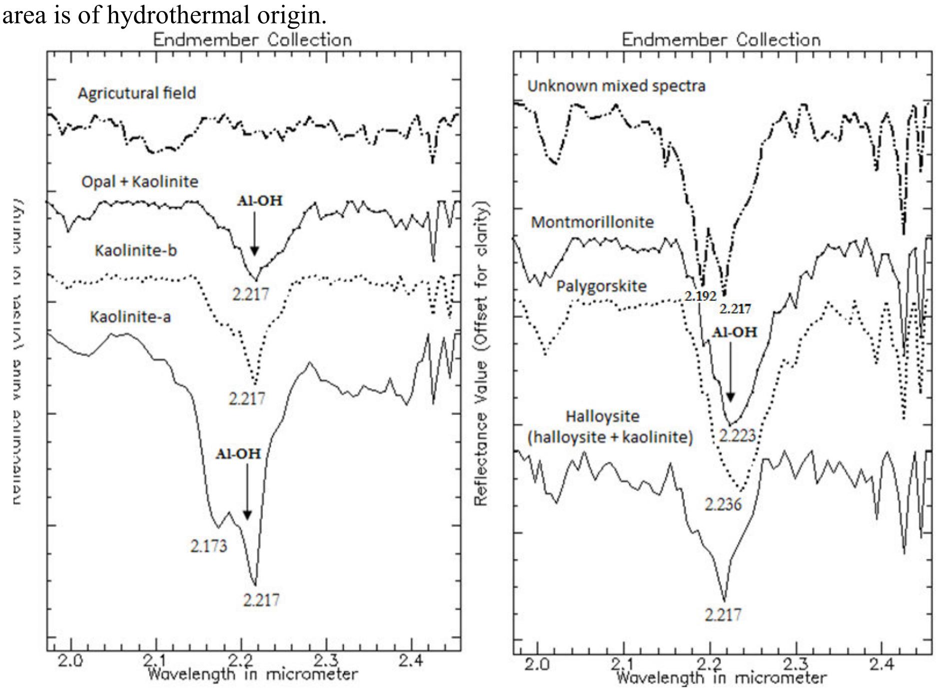

Figure 7: Image derived endmembers

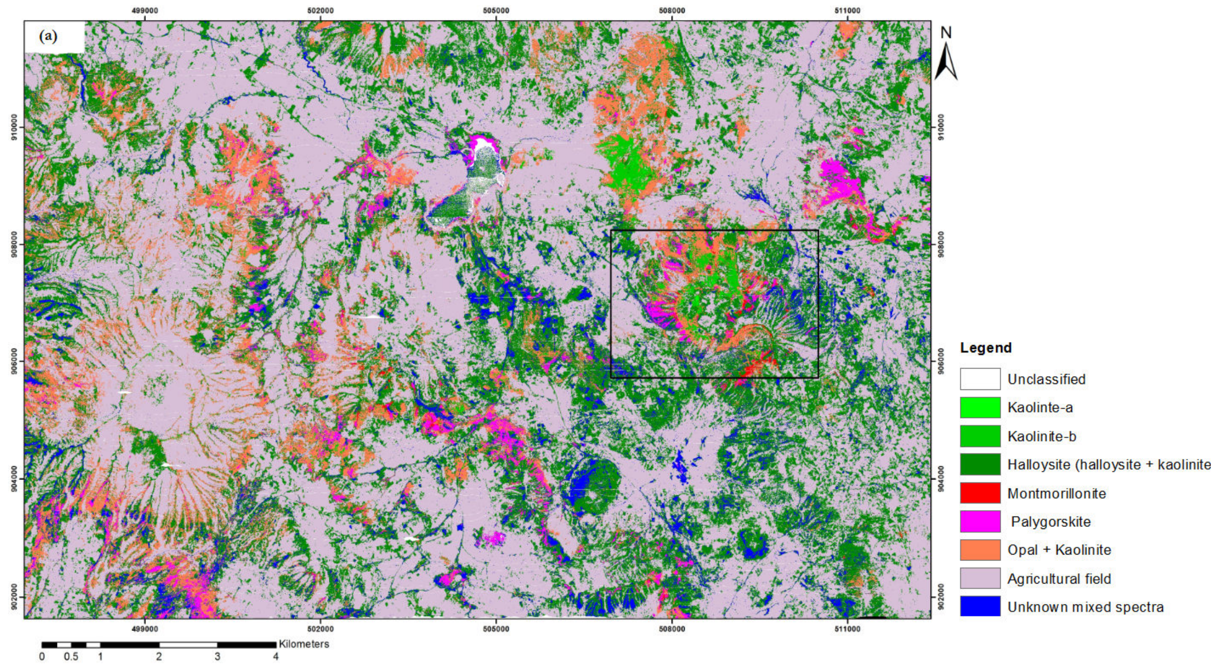

The image endmember serve as input for SAM classification algorithm. From this, surficial mineral map was generated (Figure 8a and 8b) which shows spatial distribution of the alteration mineral in the study area. Figure (8a) shows the mineral map for the entire study area while (Figure 8b) emphasis the differences in spatial distribution of the alteration areas in the detailed study area. From the surficial mineral map, kandite mineral group (kaolinite and halloysite) are mostly distributed over the study area, especially at the center of the study area where detailed study was carried out. Smectite mineral group (mainly montmorillonite) has low abundance and is sparsely distributed over the entire area. Occurrence of opal in association with kaolinite is also much in the study area. They occur in vast extent in north-eastern of the study area and at the central part (detailed study area). Palygorskite is less common over the study area in comparison with occurrence of opal and kaolinite. Palygorskite are found on the ridges, edge of the crater) (Figure 8b). Asides the alteration minerals, the agricultural field or the vegetation cover also occupy large part of the study area in which the alteration minerals occur in between. The unknown mixed spectra occur mostly on the river channel and this could probably be mixture of eroded minerals. The surficial mineral map shows the regional distribution of the alteration minerals over the study area which is not possible with the field data although the field data serves as a guide or check in picking the image endmember. From the mineral map, mineralogical zones that could relate to different hydrothermal episodes or systems could be easily recognized.

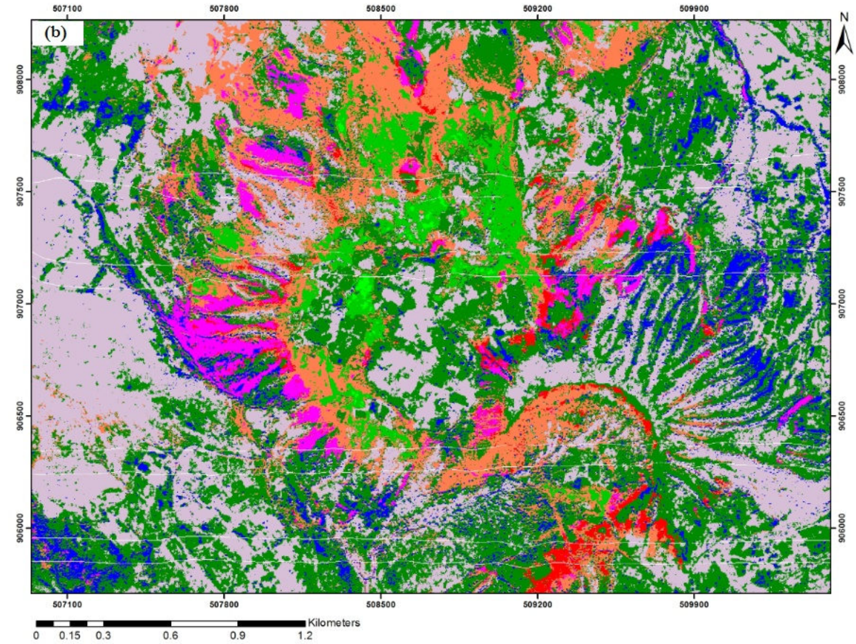

Figure 5: (a) Surficial mineral map obtained from SAM classification algorithm; (b) Zoom in of detailed study area

5. Style of Hydrothermal Alteration of Berecha Area

Hydrothermal alteration of Berecha area is strongly reflected in the bimodal volcanic rock types (rhyolite and basalt) especially on the rhyolite rock. Alteration zonation includes silicification, advanced argillic and argillic. The silicic alteration manifest in form of quartz vein (locally developed) and patches of chalcedony, without evidence of vuggy silica. This suggests a low sulfidation system (Sillitoe and Hedenquist, 2003). The most widespread alteration effects are represented essentially in advanced argillic alteration assemblage consisting mainly of kaolinite + opal + smectite $\pm$ alunite. Argillic alteration is less in the area with occurrence of some smectite $\pm$ illite. Pyrite is found as sulphide mineral in the area with absence of high sulphide minerals like enargite and luzonite, which are usually found in high sulfidation system (Table 2). Bladed calcites were found in the drill core and few occurrences at the surface with the evidence of the steaming ground. According to Hedenquist et al (2000), Steam heated water in low sulfidation environment form blankets of kaolinite, smectite, cristobalite (high-temperature polymorph of silica) and locally low alunite and native sulfur which might not have direct relationship to the ore deposit, but such blankets typically overlie the ore in the hanging wall. These characteristics features shows that Berecha area is more related to *low sulfidation system* than high sulfidation system; with low temperature of formation of about 100^0C - 300^0C and shallow depth varying between 100-600 m which is typical of low sulfidation environment (Hedenquist et al., 2000)

	Low Sulfidation	High Sulfidation
Genetically related volcanic rock	Bimodal Rhyolite to Basalt (alkali to calc-alkalic magma)	Mainly Andesite to Rhyodacite (calc-alkali magma
Fluid	Near-neutral pH, low salinity, gas-rich (CO_2, H_2S)	Acid pH, probably saline initially
Silicic alteration	Quartz vein and veinlets, silicified breccias and /or stockwork, shallow silicification, including chalcedony and/ or opaline blanket, silica sinter	Vuggy silica (residual ore bodies); partial to massive silicification; quartz vein and silicified breccias, shallow silicification, including chalcedony and/ or opaline blanket, no sinter
Advanced argillic	*Kaolinite-alunite- (illite / smectite-native sulfur) + opaline blankets of steam heated origin; commonly underlain by chalcedony blankets *Kaolinite / halloysite -alunite-jarosite blankets o zones supergene origin	*Alunite-kaolinite / dickite-pyrophyllite-diaspore of hypogene origin, typically surrounding silicic cores; also sericite pyrophyllite roots *Kaolinite-alunite blankets of steam heated or supergene origin
Argillic or Intermediate argillic	Illite / smectite halo to veins; illite + smectite halo to deeper sericite zones	Illite and illite / smectite halo to advanced argillic core
Key sulfide species	Sphalerite, galena, arsenopyrite, chalcopyrite, pyrite	Enargite, luzonite, covelite, famatinite, pyrite
Carbonate gangue	Present but typically minor	Absent
Other gangue	Barite uncommon, fluorite present locally	Barite common, typically late
Main metals	Au + Ag	Au-Ag, Cu, As- Sb
Character of mineralization	Veins common with crystalline phases at depth, banded at shallow levels	Hosted in clasts or matrix in competent wall rock alteration

6. Conclusion

Integrated analysis of both laboratory spectra from field data and SWIR hyperspectral dataset enable the identification of main alteration areas present in the study area. Mapping hydrothermal systems with imaging spectroscopy is effective and can provide detailed information. The mineral maps produced show distinctive areas of alteration which is significant in mineralization. The alteration zones area commonly associated with the structures over the study area which inferred that the spatial distribution of the alteration minerals is structurally controlled. Mount Berecha alteration system is similar to other systems that occur in some other parts of the world in terms of geological setting, alteration assemblage pattern, gangue minerals, and other features. Related features found in Berecha alteration system exists in Northern Great Basin in Western United States (John, 2001) as well as Logan creek in Australia (White et al., 1995). These systems are low-sulfidation and they host economic quantity of mineralization (mainly Au-Ag). Thus, there is possibility of mineralization in Mount Berecha alteration system, though it is not discovered at the surface based on this study. However, further study on spectra from drill core obtained from the study area will give better understanding about the alteration minerals with depth which can serve as a guide to mineral exploration in this part of the Rift System. Possible mineralization in Mount Berecha area can be traced to veins in the alteration part.

Acknowledgements

We are grateful to NERC-ARSF (Airborne Research and Survey Facility of the Natural Environment Research Council) of United Kingdom for providing the airborne data sets. Staff of Geological Survey of Ethiopia assisted us during the field work. This study was supported by Netherland Fellowship Program (NFP).

References

Abebe, B., Acocella, V., Korme, T. & Ayalew, D. (2007), Quaternary faulting and volcanism in the Main Ethiopian Rift. *Journal of African Earth Sciences,* 48**,** 115-124.

Table 3: Characteristics features of different sulfidation systems after (Sillitoe and Hedenquist, 2003)

Arthur, A. M. (2007), Field Guide for the ASD FieldSpec Pro- Raw DN Mode. National Environmental Research Council - Field Spectroscopy Facility, United Kingdom. http://fsf.nerc.ac.uk/instruments/asd_fieldspec.shtml.

Boccaletti, M., Bonini, M., Mazzuoli, R., Abebe, B., Piccardi, L. & Tortorici, L. (1998), Quaternary oblique extensional tectonics in the Ethiopian Rift (Horn of Africa). *Tectonophysics,* 287**,** 97-116.

Boccaletti, M., Mazzuoli, R., Bonini, M., Trua, T. & Abebe, B. (1999), Plio-Quaternary volcanotectonic activity in the northern sector of the Main Ethiopian Rift: relationships with oblique rifting. *Journal of African Earth Sciences,* 29**,** 679-698.

CSIRO (2010), TSG manual. *Commonwealth Scientific and Industrial Research Organisation.* Sydney, Australia.

Dipaola, G. M. (1970), Geological-Geothermal Report on the Central part of The Ethiopian Rift Valley. Ethiopia: Geological Survey Of Ethiopia.

Hecker, C. A., Van Der Meijde, M., Van Der Werff, H. M. A. & Van Der Meer, F. D. (2008), Assessing the influence of reference spectra on synthetic SAM classification results. *IEEE Transactions on geoscience and remote sensing,* Vol 46 (12)**,** pp 4162-4172.

Hedenquist, J. W., Arribas, A. R. & Gonzalez-Urien, E. (2000), Exploration for Epithermal Gold Deposits. *SEG Reviews,* 13**,** 245-277.

John, D. A. (2001), Miocene and Early Pliocene Epithermal Gold-Silver Deposits in the Northern Great Basin, Western United States: Characteristics,Distribution, and Relationship to Magmatism. *Economic Geology,* 96**,** 1827-1853.

Korme, T., Acocella, V. & Abebe, B. (2004), The Role of Pre-existing Structures in the Origin, Propagation and Architecture of Faults in the Main Ethiopian Rift. *Gondwana Research,* 7**,** 467-479.

Kruse, F. A., Lefkoff, A. B., Boardman, J. W., Heidebrecht, K. B., Shapiro, A. T., Barloon, P. J. & Goetz, A. F. H. (1993), The spectral image processing system (SIPS) - interactive visualization and analysis of imaging spectrometer data. *Remote Sensing of Environment,* 44**,** 145-163.

Pontual, S., Merry, N. & Gamson, P. (1997), Spectral Interpretation Field Manual , Spectral Analysis Guide for Mineral Exploration, G-MEX Vol 1, AusSpec International.

Reed, M. (1997), Hydrothermal alteration and its relationship to ore fluid composition. *Geochemistry of hydrothermal ore deposits.* John Wiley and Sons, Inc.

Sillitoe, R. & Hedenquist, J. W. (2003), Linkages between Volcanotectonic settings, Ore-Fluid Compositions, and Epithermal Precious Metal Deposits. *SEG Newsletter,* Special Publish 10**,** 315-343.

Tadesse, S. (1999), Geology and Gold Mineralization in the Pan-African Rocks of the Adola Area, Southern Ethiopia. *Gondwana Research,* 2**,** 439-447.

Tadesse, S., Milesi, J.-P. & Deschamps, Y. (2003), Geology and mineral potential of Ethiopia: a note on geology and mineral map of Ethiopia. *Journal of African Earth Sciences,* 36**,** 273-313.

Thomas, M. & Walter, M. R. (2002), Application of Hyperspectral Infrared Analysis of Hydrothermal Alteration on Earth and Mars. *Astrobiology,* Volume 2, No 3.

Trua, T., Deniel, C. & Mazzuoli, R. (1999), Crustal control in the genesis of Plio-Quaternary bimodal magmatism of the Main Ethiopian Rift (MER): geochemical and isotopic (Sr, Nd, Pb) evidence. *Chemical Geology,* 155**,** 201-231.

Tsegaye, A., Manetti, P., Bonini, M., Corti, G., Innocenti, F., Mazzarini, F. & Pecksay, Z. (2005), Geological map of the northern Main Ethiopian Rift and its implications for the volcano-tectonic evolution of the rift.

van der Meer, F. (2001), *Basic Physics of Spectrometry, Chapter 1 of Imaging Spectrometry: Basic Principles and Prospective Applications*, Kluwer Academic Publishers, Netherlands.

Van Der Meer, F. D., Van Der Werff, H. M. A., F.J.A., V. R., C.A., H., W.H., B., M.F., N., M., V. D. M., E.J.M., C., De Smeth, J. B. & Woldai, T. (2012), Multi - and hyperspectral geologic remote sensing : a review. *International Journal of Applied Earth Observation and Geoinformation,* Vol 14 (1)**,** pp. 112-128.

White, N. C., Leake, M. J., Mccaughey, S. N. & Parris, B. W. (1995), Epithermal gold deposits of the southwest Pacific. *Journal of Geochemical Exploration,* 54**,** 87-136.

Woldegabriel, G., Aronson, J. L. & Walter, R. C. (1990), Geology, geochronology, and rift basin development in the central sector of Main Ethiopia Rift. *Geological Society of America Bulletin,* v. 102**,** 439-458.